Jurnal Kejuruteraan 32(3) 2020: 455-465
https://doi.org/10.17576/jkukm-2020-32(3)-10

Ultra-Wideband Planar Antenna with Notched-Band for WIMAX, WLAN and MSAT Applications

Siti Fatimah Jainal*
Malaysia-Japan International Institute of Technology (MJIIT), UTM Kuala Lumpur, Malaysia
Faculty of Engineering, Lincoln University College, Malaysia

Norliza Mohamed
Razak School of Engineering and Advanced Technology, UTM Kuala Lumpur, Malaysia

Azura Hamzah
Malaysia-Japan International Institute of Technology (MJIIT), UTM Kuala Lumpur, Malaysia

Suhaila Subahir
Centre for Communication Engineering Studies, Universiti Teknologi MARA (UITM Shah Alam), Selangor, Malaysia

**Corresponding author: lincolnsfj@gmail.com*

Received 22 October 2020, Received in revised form 29 March 2020
Accepted 30 April 2020, Available online 30 August 2020

ABSTRACT

Ultra-wideband (UWB) with triple band notch characteristics was presented. WIMAX, WLAN and Meteorological Satellite (MSAT) frequency bandwidths were rejected in the UWB planar antenna composed from a single layer conductor element. Frequency bandwidths for WIMAX, WLAN and MSAT are allocated at 3.3~3.7, 5~6 and 7.4~8.4GHz, respectively. Conductor element etching method was used as the means to realize the band notch characteristics as it was considered convenient and simple. Two slits were etched on the ground plane while on the elliptical element, a single slit. The slits were designed for simplicity in the means of achieving the desired band notch characteristics. The proposed antenna design was compact and low profile. The antenna performances were compared with the reference antenna and the results were negligible.

Keywords: Ultra-wideband; WIMAX; WLAN; MSAT; Slit; Elliptical element

INTRODUCTION

Ultra-wideband (UWB) applications have been established since the 1950s. It has been used for wireless transporting of voice, video, and data. UWB communication systems are applied in medical institutions for detection of breast cancer (LiXu et al. 2013), wave propagation for calculating the impulse response by using ray tracing techniques and inverse Fourier transform (Chen et al. 2006), civil engineering for construction to investigate and emphasize the effects of the industry operation (Shaohua et al. 2011), and robotic engineering for mobile robot localization by determining the space to a position of joined and well-neighboring beacons (Gonzales et al. 2009).

Furthermore, UWB application is also found in network engineering to propose scattering protocol for portable radios provided with impulse-ultra wideband (I-UWB) (Farshad et al. 2008), biomedical engineering to identify the movements of each finger muscle (Mohamed, 2010) and automation engineering to enable and establish accuracy to locate and estimate the presence of metal objects (Maalek and Sadeghpour, 2012).

UWB is suitable for the identification and tracking of construction resources (Siddiqui et al. 2019). UWB antenna systems have also been used as in-body implantable antennas in the human body that could communicate with nearby base stations as well as for multiple biotelemetric applications (Abdul & Hyoungsuk, 2019).

However, UWB communication systems coexist with other communication systems such as WIMAX, WLAN and Meteorological Satellite, which are allocated between the frequency bandwidth of 3.3~3.7, 5~6 and 7.4~8.4 GHz, respectively. Coexisting frequency bandwidths could result in interferences. UWB also coexists with the frequency bandwidth of mobile services operating at 3.4 to 3.8 GHz and has shown potential interferences to the UWB system (Dmytro et al. 2019). These interferences could result in multipath fading of radio frequency in the industrial and factory environment (Jose et al. 2009), obstruct a radio communication services in computer networking (Bazil et al. 2010), degrade WLAN and WSN when operating simultaneously (Abdullah et al. 2011), decay metrological performance and incite disturbance effects (Giovanni et al. 2010) and cause biomedical devices malfunction (Phond et al. 2010).

Devices are subjected to certain rules such as the device must not cause harmful interference and must accept any interference received. Thus, it is essential to eliminate potential interference in communication system devices.

Several examples for previously studied UWB communication systems with band rejections have been presented. UWB planar antennas with band notch characteristics to reject frequency bandwidth between 5 and 6 GHz have been discussed (Bhattacharya et al. 2019) (Jainal et al. 2019). Band rejections for frequency bandwidths at 5 to 6 GHz and 3.3 to 3.7 GHz, by using slits in the conductor elements have also been studied (Jainal et el., 2019). Band rejections for frequency bandwidths 3.3 to 3.7 GHz and 5 to 6 GHz have been generated by an L-shaped and split ring resonator (SRR) (Mohamed et al. 2019).

The reference and proposed antenna structure are presented in the methodology section and the antenna performances are discussed in the result section. The study is then concluded in the conclusion section.

METHODOLOGY

UWB PLANAR ANTENNA WITH TRIPLE BAND NOTCH CHARACTERISTICS

The reference and the antenna parameters are presented in Figure 1 and tabulated in Table 1. Reference antenna is a UWB planar antenna comprising an elliptical radiator. The reference antenna used a half-ground plane with an elliptical element on top of the substrate. The impedance matching for the reference antenna was determined by the eccentricity, e as shown in Equation (1) and the space flanked by the elliptical radiator and the ground. The major L_1 and minor L_2 are diameters for the elliptical element for eccentricities $e\approx0$, $e\approx1$ and $e\approx0.6$.

A coaxial cable was used as the feeding line and was soldered on top of the ground plane from the bottom edge of the elliptical element with feed of 50 Ω. The type of port used in the simulation was a coaxial waveguide port and located in the feed point of the elliptical element. Modes in the coaxial waveguide port were polarized.

The reference and UWB planar antenna type 3A1 and 3A2 were analyzed in Computer Software Technology (CST) software Microwave component (Microwave, RF and Optical) for Antenna (Planar) applications. The simulation ran in transient solver between 3 and 11 GHz in the open space boundary condition and convolution PML of 0.0001 to minimize the reflections from the boundary condition. The antennas were simulated in far-field, which is an in-plane wave propagation. Simulation setup for the reference and UWB planar antenna type 3A1 and 3A2 are illustrated in Table 2.

Reference antenna was reconfigured to generate the triple band notch characteristics. UWB planar antenna type 3A1 and 3A2 with three slits S_1, S_2 and S_3, etched horizontally on the conductor elements were designated as the proposed antenna and illustrated in Figure 2. Slit structures and dimensions are listed in Figure 3 and Table 3, accordingly. Slit S_1 was etched in the elliptical element, whereas S_2 and S_3 were in the ground plane.

Slit parameters include slit length l, width w and slope angle, θ. Slit S_1, S_2 and S_3 parameters for UWB planar antenna type 3A1 and 3A2 were indicated by $S_{1(3A1)}$, $S_{1(3A2),}$ $S_{2(3A1),}$ $S_{2(3A2),}$ $S_{3(3A1)}$ and $S_{3(3A2)}$, respectively. Theoretically,

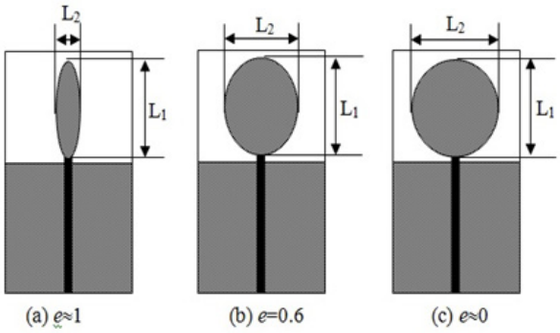

FIGURE 1. Reference Antenna Eccentricity, e

TABLE 1. Parameters for Reference, UWB Planar Antenna Type 3A1 and 3A2

Parameter	Dimension
Substrate thickness h_s	1.6 mm
Conductor plane thickness h_c	0.035 mm
Coaxial cable length L_{cable}	47 mm
Major diameter (elliptical) L_1	16 mm
Minor diameter (elliptical) L_2	12.8 mm
Length for ground plane L_g	24 mm
Width for ground plane W_g	21 mm
Length for substrate L_s	45 mm
Width for substrate W_s	21 mm
Substrate permittivity ϵ	4.6
Tangent delta electric (substrate conductivity)	0.019

TABLE 2. Simulation Setup for Reference, UWB Planar Antenna Type 3A1 and 3A

Parameter	Value
Frequency f	3~11 GHz
Reflection coefficient S_{11}	<-10 dB
Convolution PML	0.0001
Boundary	Open space
Band notch BN1	f_{BN1} = 5~6 GHz, S_{11} >-10 dB
Band notch BN2	f_{BN2} = 3.3~3.7 GHz, S_{11} >-10 dB
Band notch BN3	f_{BN3} = 7.4~8.4 GHz, S_{11} >-10 dB

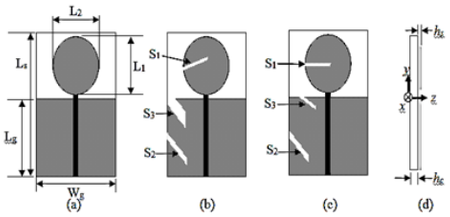

FIGURE 2. UWB Planar Antenna Structures (a) Reference (b) Type 3A1 (c) Type 3A2 (d) Side view

slits were used to change the input impedance of the UWB planar antenna type 3A1 and 3A2.

Slit S_1 was etched on the elliptical radiator in the first simulation stage to achieve band notch characteristics for the frequency bandwidth f_{BN1} = 5~6 GHz. Later, second and third slits S_2 and S_3 were etched on the ground plane in order to achieve the second and third band notch of BN2 and BN3, consecutively.

Reflection coefficient S_{11} changed due to the disruption in the exterior current stream in the elliptical radiator and ground plane, hence band notch characteristics were generated. Desired band notch characteristics were obtained when the slit parameters were changed. Theoretically, the slit angle Θ can be adjusted in improving the reflection coefficient S_{11} between the desired notched-band frequency.

Band notch characteristic that was generated by slit S_1, S_2 and S_3 were known as the BN1, BN2 and BN3, respectively. Band notch characteristics were classified into three parameters; frequency bandwidth f_{BN}, peak of reflection coefficient S_{11} and center frequency f_c, respectively. Parameters for slit length l, width w and slope angle θ for slit S_1, S_2 and S_3 were optimized in the means to achieve the optimum band notch characteristics.

RESULTS AND DISCUSSION

REFLECTION COEFFICIENT S_{11}

Reflection coefficient S_{11} for the eccentricity e is illustrated in Figure 5. Reflection coefficient S_{11} when eccentricity e≈1 and e≈0 were mismatched, which was above -10 dB level between the frequency bandwidth $f_{(e\approx1)}$=3.31~8.35, 8.79~11GHz and $f_{(e\approx0)}$=4.33~4.91, 7.26~8.72 GHz. However, reflection coefficient S_{11} was below -10 dB level for the frequency bandwidth $_{f(e=0.6)}$= 3~11 GHz, which meant that the antenna was radiating below this level. Thus, the eccentricity e=0.6 was selected for impedance matching with respect to the reference antenna as the reflection coefficient S_{11} between the frequency 3 and 11 GHz was below -10 dB.

Reflection coefficient S_{11} for the reference, UWB planar antenna type 3A1 and 3A2 were optimized, consecutively. Optimization was carried out by using simulation setup in CST software. The slit parameters were set to change their dimensions by referring to the reflection coefficient S_{11} value that must achieve less than -5 dB range.

$$e = \sqrt{1 - \left(\frac{L_2}{L_1}\right)^2} \tag{1}$$

Slit S_1, S_2 and S_3 parameters were modified and optimized to generate the band notch BN1, BN2 and BN3 in the desired frequency bandwidths. Optimized simulated reflection coefficient S_{11} were compared with the measured data and illustrated in Figure 6 and Table 4.

The comparisons were reasonable. Tolerance (%) between simulated and measured band notch characteristics were significantly small and thus considered negligible. The differences between simulation and measurement results were possibly due to the fabrication and soldering factor. Furthermore, experimental conduct such as noise, and connectors used from the fabricated models to the measuring equipment (turntable/network analyzer) could also contribute to the result differences.

Maximum reflection coefficient S_{11} for band notch BN1 and BN3 for UWB planar antenna type 3A1 was slightly lower than type 3A2. However, maximum reflection coefficient S_{11} for band notch BN2 for UWB planar antenna type 3A2 was lower than type 3A1.

The difference was due to the position of slit S_1, which was on the elliptical element. Slit S_1 in the proposed antenna type 3A1 and 3A2 was placed at the center of the elliptical radiator. However, slit S_1 for the proposed antenna type 3A2

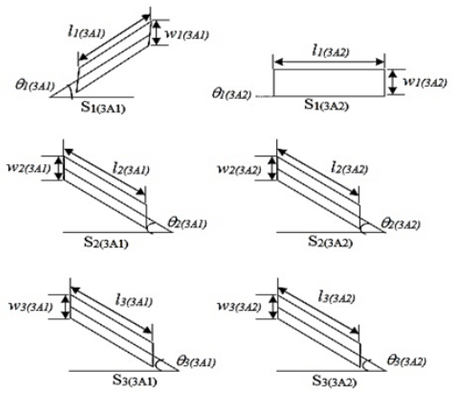

FIGURE 3. Slit Structure for S_1, S_2 and S_3

TABLE 3. Slit Parameters for S_1, S_2 and S_3

Antenna type	Slit	Parameter	Dimension
3A1	S_1	l_1	6.49 mm
		w_1	2.30 mm
		Θ_1	4.33 mm
	S_2	l_2	11.01 mm
		w_2	0.60 mm
		Θ_2	39.47 deg
	S_3	l_3	6.32 mm
		w_3	3.00 mm
		Θ_3	50.77 deg
3A2	S_1	l_1	6.77 mm
		w_1	1.10 mm
		Θ_1	0.00 deg
	S_2	l_2	11.00 mm
		w_2	0.60 mm
		Θ_2	39.43 deg
	S_3	l_3	5.34 mm
		w_3	5.34 mm
		Θ_3	29.49 deg

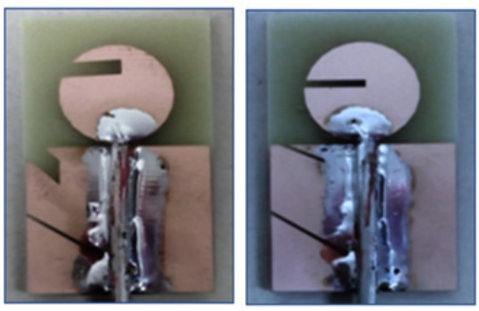

(a)Type 3A1 (b) Type 3A2

FIGURE 4. Prototype for UWB Planar Antenna

was slightly in the lower fraction of the elliptical radiator when compared to type 3A1. Exterior current distribution was more converged in the lower part. Thus, surface current was more distributed in slit S_1 for UWB planar antenna type 3A2 as compared to type 3A1.

EXTERIOR CURRENT DISTRIBUTION

Exterior current distributions for the reference, proposed antenna type 3A1 and 3A2 are illustrated in Figure 7. The center frequencies f_c = 3.5, 5.5, 8 GHz were determined at the peak of the reflection coefficient S_{11} for band notch BN1, BN2 and BN3, respectively. The exterior current distributions for UWB planar antenna type 3A1 and 3A2 were compared with the reference antenna to investigate the relation between the input impedance mismatch and slits S_1, S_2 and S_3.

For the reference antenna, surface current was saturated in the feed, edge and upper parts of ground plane in the frequency f=3.5 GHz. Surface current in the lower fraction of the elliptical radiator was more condensed than the upper part. Saturation of surface current was more intense in the feed, upper, edges and lower parts of the ground at the frequency f=5.5 GHz.

Surface current was intensely condensed in the elliptical radiator, edges and the upper fraction of the ground in the frequency f=8 GHz. Surface current was most saturated in the feed area.

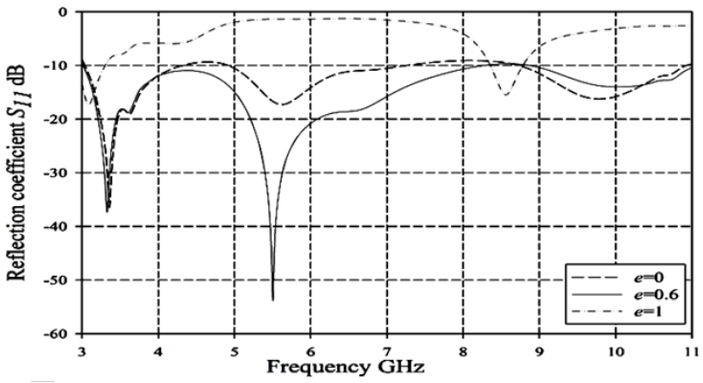

FIGURE 5. Reflection Coefficient S_{11} for Eccentricity, e

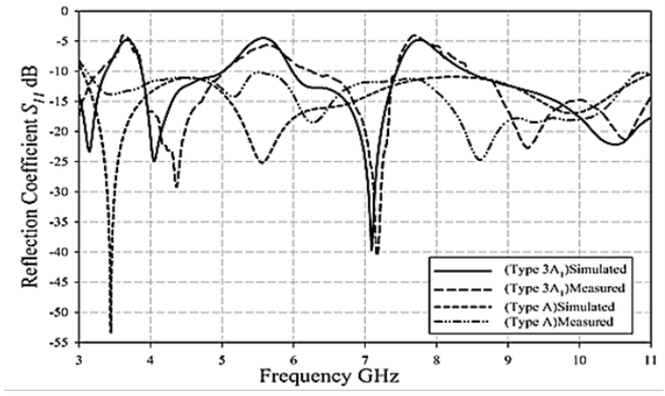

(a) Type 3A1

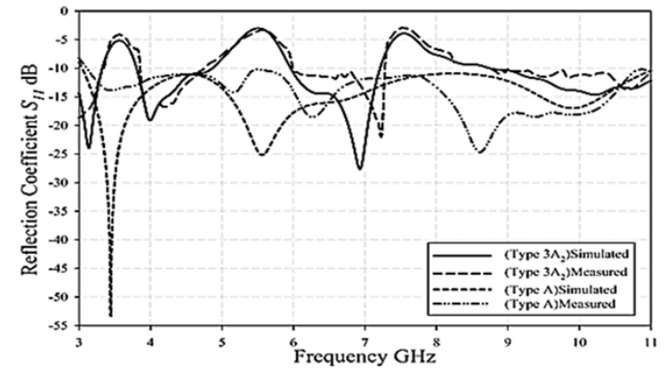

(b) Type 3A2

FIGURE 6. Simulated and Measured for Reflection Coefficient S_{11} UWB Planar Antenna

The exterior current in the upper area of the ground plane was highly condensed due to its short distance to the feed. Exterior current stream was in perpendicular. The exterior current flow at the cutting edges was extended exponentially in the ground plane and elliptical element. Thus, slit was etched parallel on the elliptical radiator and the ground as a means to interrupt the vertical exterior current flow.

For UWB planar antenna type 3A1 and 3A2, surface currents were distributed in slit S_1, S_2 and S_3 in the frequency f_c =5.5, f_c= 3.5 and f_c = 8 GHz. Thus, it was considered that saturation of exterior current in a particular slit had generated the impedance mismatch and band notch characteristics in the respective frequencies.

Maximum exterior current distributions for reference, proposed antenna type 3A1 and 3A2 were studied. Maximum surface current distributions for reference, proposed antenna type 3A1 and 3A2 were given I_{ref} = 141.8 A/m, I_{3A1} = 322.7 A/m and I_{3A2} = 296.1 A/m at the frequency f_{ref} = 5.5 GHz, f_{3A1} = 3.5 GHz and f_{3A2} = 5.5 GHz, respectively.

TABLE 4. Band Notch Characteristics BN1, BN2 and BN3 Comparison between Simulated and Measured Reflection Coefficient S_{11} for UWB Planar Antenna

Antenna type	Band notch	Frequency bandwidth fb_w GHz			Center frequency GHz			Maximum reflection coefficient S_{11} dB		
		Simulated	Measured	Tolerance %	Simulated	Measured	Tolerance %	Simulated	Measured	Tolerance %
3A1	BN1	1.00 (5.00~6.00)	1.10 (5.00~6.10)	0.1	5.57	5.60	0.005	-4.50	-3.02	0.3
	BN2	0.40 (3.30~3.70)	0.41 (3.31~3.70)	0.025	3.60	3.55	0.01	-4.70	-5.00	0.06
	BN3	1.00 (7.40~8.40)	1.00 (7.40~8.40)	0.0	7.70	7.54	0.02	-4.70	-3.90	0.17
3A2	BN1	1.00 (5.00~6.00)	1.05 (4.95~6.00)	0.05	5.51	5.53	0.003	-5.90	-3.00	0.5
	BN2	0.40 (3.30~3.70)	0.45 (3.30~3.75)	0.125	3.56	3.55	0.002	-4.60	-3.5	0.2
	BN3	1.00 (7.40~8.40)	1.10 (7.45~8.55)	0.1	7.54	7.58	0.005	-3.90	-3.50	0.1

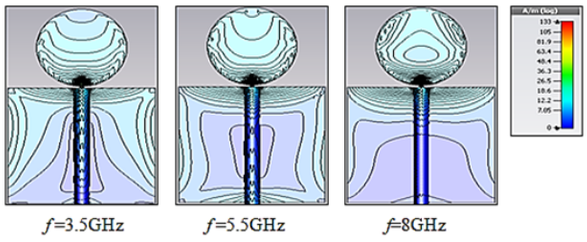

(a) Reference antenna

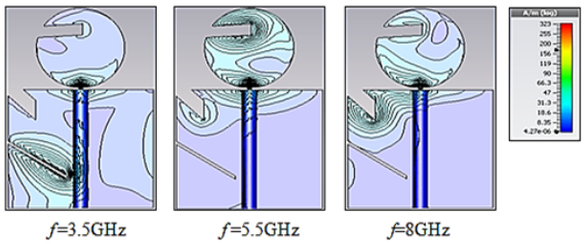

(b) Type 3A1

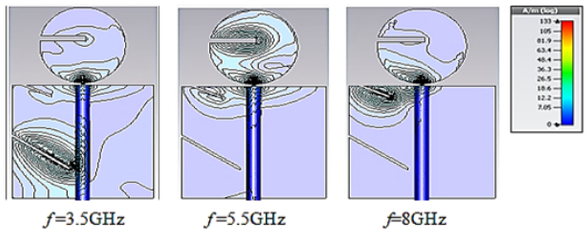

(c) Type 3A2

FIGURE 7. Surface Current Distribution

RADIATION PATTERN RP

Radiation patterns for proposed antenna type 3A1 and 3A2 are illustrated in Figure 8. Frequency of interest were chosen at f=4.5, 6.5 and 9.5GHz as it was taken in the interval between the notched frequencies, which were at 3.3~3.7, 5~6, and 7.4~8.4 GHz. The UWB frequency bandwidth is allocated between 3.1~10.6 GHz and then divided into three sections that are lower (3.1~5.5 GHz), middle (5.5~8 Ghz) and higher (8~10.6 GHz) frequency regions. Radiation patterns in the H- and E-plane of type 3A1 and 3A2 were in omni- and bi-directional, respectively. Number of lobes was increased in the E-plane due to the ratio of wavelength

λ to the frequency *f*. It was considered that the slit S_1 in the elliptical element had affected the radiation pattern in the E-plane at the frequency *f*=6.5 GHz.

Radiation patterns for the reference antenna in the E-plane was symmetrical as the structure of the antenna was not modified. However, the E-plane was affected when slit S_1 was etched on the elliptical radiator in the parallel position.

Thus, the parallel etched slits disrupted the vertical E-plane radiation patterns. The H-plane was not significantly affected as the slits were etched horizontally. From the frequency of interest, maximum gain $G_{max(3A1)}$=6.6 dB and $G_{max(3A2)}$=6.1 dB were obtained in the H- and E-plane of θ=175 deg and φ=162 deg, and θ=181 deg and φ=162 deg at the frequency *f*=4.5 GHz for type 3A1 and 3A2, respectively.

However, lowest gain $G_{min(3A1)}$=3.5 dB and $G_{min(3A2)}$=3.4 dB were at the frequency *f*=9.5 GHz for θ=150 deg and φ=127 deg, and θ=127 deg and φ=132 deg for type 3A1 and 3A2, respectively. Maximum gain *G* for type 3A1 and 3A2 were found in the *–z* –axis for the H-plane for the frequency *f*=4.5, 9.5 GHz. However, for the E-plane the maximum gain *G* were at +*y* –axis for the frequency *f*=4.5, 9.5 GHz, and at *–y* –axis for the frequency *f*=6.5 GHz, respectively.

GAIN *G* AND RADIATION EFFICIENCY E_{RAD}

Simulated and measured maximum gain *G* and efficiency e_{rad} for the reference, UWB planar antenna type 3A1 and 3A2 are presented in the Figure 9. Tolerance % between the simulated and measured gain *G* and efficiency e_{rad} were significantly small. Gain *G* and efficiency e_{rad} at the band notch center frequency f_c BN1, BN2 and BN3 are tabulated in Table 5. Simulated maximum gain *G* for the reference, proposed antenna type 3A1 and 3A2 were at the frequency $f_{(ref)}$=9.2 GHz, $f_{(3A1)}$=10.7 GHz and $f_{(3A2)}$=10.9 GHz for $G_{max(ref)}$=5.2 dB, $G_{max(3A1)}$=6.5 dB and $G_{max(3A2)}$=7.8 dB, respectively. Radiation efficiency e_{rad} at the frequency *f*=3.5, 3.6, 5.6, 7.9, 7.8 GHz for the UWB planar antenna type 3A1 and 3A2 were lower than the reference antenna. The frequency bandwidths were allocated within the band notch characteristics of BN1, BN2 and BN3, respectively.

Lowest radiation efficiency e_{rad} was at the frequency *f*=7.98 GHz with e_{rad}=41.9% for UWB planar antenna type 3A2. Overall, radiation efficiency e_{rad} cliffs at the band notch frequency bandwidths for type 3A2 were lower than type 3A1. Thus, it was considered that slits in the elliptical radiator and ground affected the radiation efficiency e_{rad} and the slits that were etched in UWB planar antenna type 3A2 were more efficient to generate the band notch characteristics.

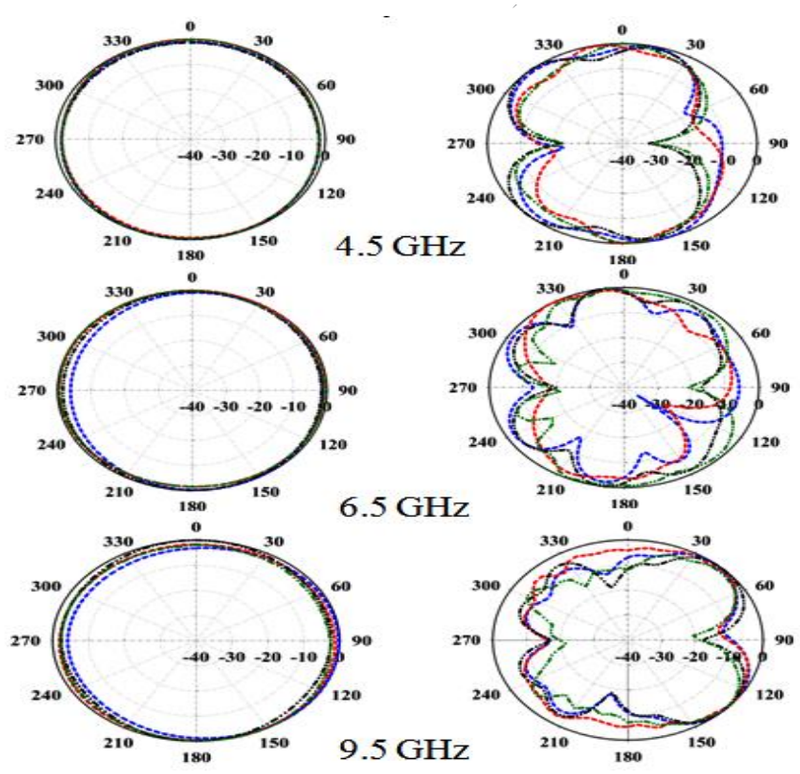

(a) Type 3A1

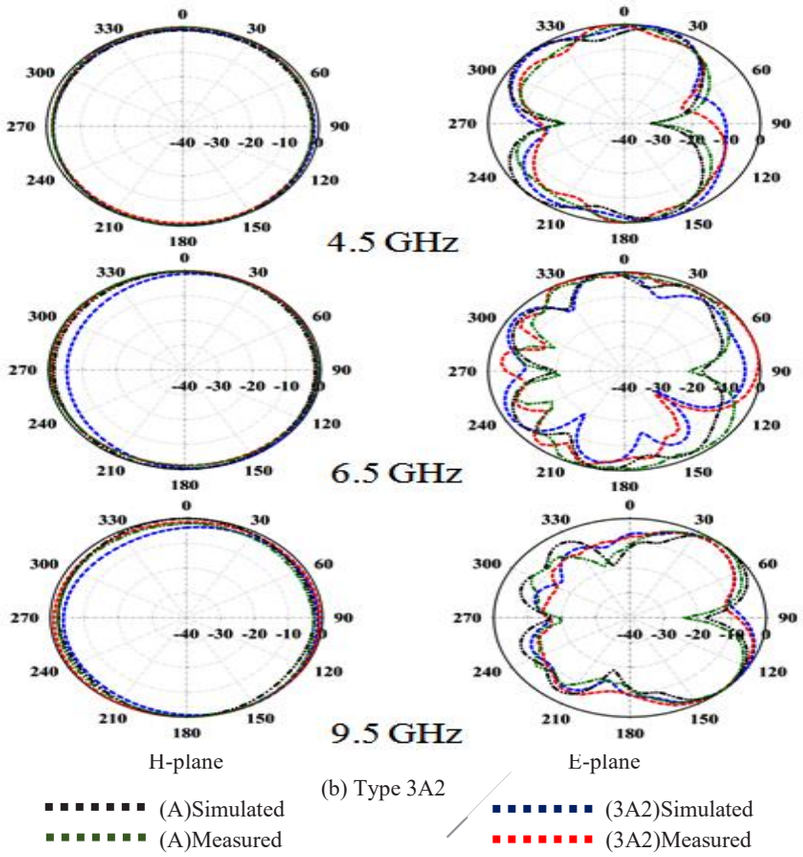

FIGURE 8. Radiation Patterns for UWB Planar Antenna

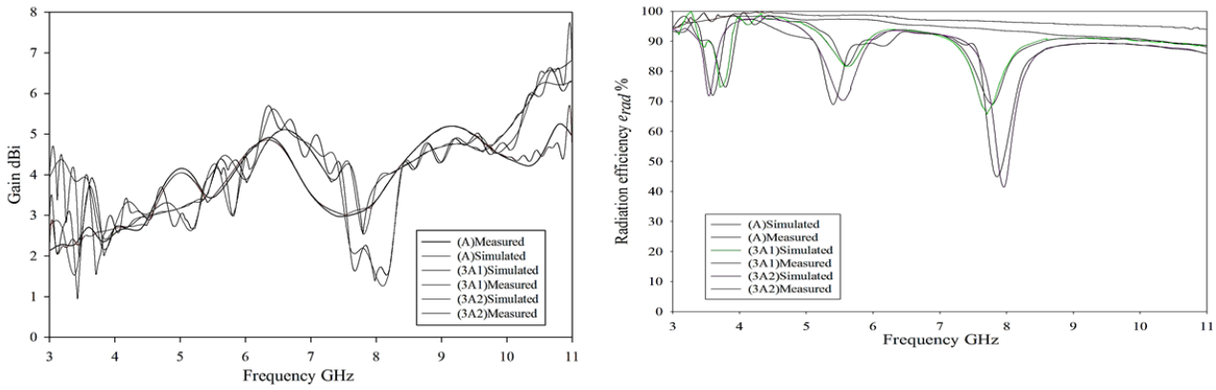

(a) Maximum gain G (b) Radiation efficiency e_{rad}

FIGURE 9. UWB Planar Antenna Type 3A1 and 3A2 for (a) Maximum gain *G* (b) Radiation efficiency e_{rad}

TABLE 5. Gain *G* and Radiation Efficiency e_{rad} for Band Notch BN1, BN2 and BN3 Characteristics of UWB Planar Antenna Type 3A1 and 3A2

Band notch	Antenna type/Band notch characteristics		A	Tolerance %	3A1	Tolerance %	3A2	Tolerance %
BN1	Centre frequency fc	Simulated	5.60	0.0	5.60	0.0	5.55	0.02
		Measured	5.60		5.60		5.39	
	Gain G	Simulated	3.55	0.01	4.36	0.04	4.33	0.18
		Measured	3.6		4.15		3.55	
	Radiation efficiency erad	Simulated	97.24	0.01	81.58	0.004	70.61	0.01
		Measured	98.67		81.95		69.91	
BN2	Centre frequency fc	Simulated	3.60	0.0	3.61	0.05	3.53	0.01
		Measured	3.60		3.80		3.60	
	Gain G	Simulated	2.40	0.03	3.62	0.07	4.14	0.05
		Measured	2.48		3.89		3.91	
	Radiation efficiency erad	Simulated	97.73	0.01	74.89	0.002	71.92	0.002
		Measured	96.67		74.70		72.06	
BN3	Centre frequency fc	Simulated	7.88	0.0	7.89	0.02	7.88	0.003
		Measured	7.88		7.71		7.85	
	Gain G	Simulated	3.31	0.03	4.35	0.14	2.19	0.12
		Measured	3.18		3.71		1.91	
	Radiation efficiency erad	Simulated	94.65	0.02	66.09	0.04	41.96	0.07

TABLE 6. Comparisons with other UWB Planar Antenna Design with Triple Band Notch Characteristics

Reference	Size (mm2)	Band notching method	Notched frequencies (GHz)	Drawback
Wang, S., Dong, J. &Wang, M.	35.5x30	Arc-H and L-, and T-shaped slot	Wimax 3.3~4.68 Wlan 5.15~6.48 X-band 7.25~8.54	Design complexity.
Ain, Q. & Chattoraj, N.	31x24	Multiple C-shaped slots	Wimax 3.3~3.7 Upper Wlan 5.7~6 Lower Wlan 5.1~5.4	Design complexity.
Elhabchi, M., Srifi, M.N. & Touahmi, R.	26x26	Inverted T- and I-shaped slots, and dual split ring resonators.	5G 3.3~3.7 Wlan 5.72~5.84 X-band 7.1~8.39	Bulky design.
Kumar, S. & Khan, T.	25x30	U- and Archimedean spiral shaped EBG unit cells	Insat 4.5 Wlan 5.1 Radio 9.1	Bulky design.
Kumar, O.P., Singh, A., Sinha, R. & Ali, T.	30x30	Semi-and quarter circular slots, and EBG	Wimax 3.1~3.8 Wlan 5.3~5.8 C-band 6.9~7.5	Bulky design.
Faouri, Y.S., Awad, N.M. & Abdelazeez, M.K.	36x36	Inverted E-stub, dual triangular slots and a square slot	Wimax 1.66~3.29 Wlan 4.72~5.81 X-band 7.86~8.62	Bulky design.
Khattak, M.I., Khan, M.I., Ullah, Z., Ahmad, G. & Khan, A.	30x28	Rectangular, U-and inverted U-shaped slots.	Wimax 3.1~3.7 Wlan 5.1~5.8 ITU-band 7.95~8.4	Design complexity.
Proposed antenna	45x21	Triple slits	Wimax 3.3~3.7 Wlan 5~6 MSAT 7.4~8.4	Design simplicity.

Slit S_3 was etched in the upper part of the ground plane and near to the feed. Thus, at the frequency bandwidth f=7.4~8.4 GHz, the surface current distribution in the elliptical radiator and ground were mostly disrupted and the maximum gain G and the radiation efficiency e_{rad} were significantly changed.

CONCLUSION

UWB planar antenna with triple band notch characteristics has been recommended and studied. The designed antennas were compact and low profile. Etching was regarded as to create the band notch characteristics in a simple way. Slits in the elliptical radiator and ground were etched as to create the band notch characteristics for the frequency bandwidth to eliminate WLAN, WIMAX and MSAT communication system. Slits S_1, S_2 and S_3 in the elliptical radiator and ground were to create band notch characteristics between the frequency bandwidth 5~6, 3.3~3.7 and 7.4~8.4 GHz, respectively. The proposed antenna performances such as reflection coefficient S_{11}, surface current distribution, gain G and efficiency e_{rad} were compared with the reference antenna and the results were reasonable.

DECLARATION OF COMPETING INTEREST

None.

ACKNOWLEDGEMENT

Research was financially supported by Universiti Teknologi Malaysia (UTM) Razak grant fund vote No. 05G58. Antenna measurements were conducted in Antenna Research Center (ARG), Faculty of Engineering (FOE), Universiti Teknologi Mara (UITM-Shah Alam).

REFERENCES

Ain, Q. & Chattoraj, N. 2018. Parametric study and analysis of band stop characteristics for a compact uwb antenna tri-band notches. *Journal of Microwave, Optoelectronics and Electromagnetic Application* 17(4):509-527.

Abdul, B. & Hyoungsuk, Y. 2019. A stable impedance-matched ultrawideband antenna system mitigating detuning effects for multiple biotelemetric applications. *IEEE Transactions on Antennas and Propagation* 67(5):3416-3421.

Ahmed, B.T., Campos, J.L.M. & Cruz, J.R.A. 2010. Impact of ultra-wide band emission on wimax systems at 2.5 and 3.5 GHz. *Elsevier Computer Networks* 54(10):1573-1583.

Betta, G., Capriglione, D., Ferrigno, L. & Miele, G. 2010. Influence of wi-fi computer interfaces on measurement apparatuses. *IEEE Transactions on Instrumentation and Measurement* 59(12):3244-3252.

Bhattacharya, A., Roy, B., Chowdhury, S.K. & Bhattacharjee, A.K. 2019. Compact printed ultra-wideband monopole antenna with band-notch characteristics. *Indian Journal of Pure & Applied Physics (IJPAP)* 57(2019):272-277.

Chen, C.H., Liu, C.L., Chiu, C.C. & Hu, T.M. 2012. Ultra-wide band channel calculation by sbr/image techniques for indoor communication. *Taylor & Francis Journal of Electromagnetic Waves and Applications* 20(1):41-51.

Cui, L., Liu, H., Hao, C. & Sun, X. 2019. A novel uwb antenna with triple band-notches for wimax and wlan. *Progress in Electromagnetic Research Letters* 82:101-106.

Chilo, J., Karlsson, C., Angskog, P. & Stenumgaard, P. 2009. Emi disruptive effect on wireless industrial communication systems in a paper plant. *IEEE International Symposium on Electromagnetic Compatibility 2009,*151-154.

Dmytro, M., Rostyslav, B., & Olena, O. 2019. Interference from ultra-wideband devices on mobile service in the frequency range of 3400-3800MHz. *Conference ELNANO* (*IEEE 39th International Conference on Electronics and Nanotechnology)2019,* 563-567.

Doddipalli, S. & Kothari, A. 2019. Compact uwb antenna with integrated triple notch bands for wban application. *IEEE Access* 7(2019):184-190.

Dong, J., Zhuang, X. & Hu, G. 2018. Planar uwb monopole antenna with tri-band rejection characteristics at 3.5/5.5/8 GHz. *Information* 2019 (10):1-11.

Eldosoky, M.A.A. 2010. Classification of finger movements by using the ultra-wideband radar. *Taylor & Francis Computer Methods in Biomechanics and Biomedical Engineering* 13(6):865-868.

Elhabchi, M., Srifi, M.N. & Touahni, R. 2019. Cpw-fed miniaturized isosceles triangular slot uwb planar. *Progress in Electromagnetics Research Letters* 87:59-66.

Faouri, Y.S., Awad, N.M. & Abdelazeez, M.K. 2019. Hexagonal patch antenna with triple band rejections. *Conference JEEIT (IEEE Jordan International Joint Conference on Electrical Engineering and Information Technology) 2019*, 446-448.

Gonzalez, J., Blanco, J.L., Galindo, C., Galisteo, A.O.D., Madrigal, F.J.A., Moreno, F.A. & Martinez, J.L. 2009. Mobile robot localization based on ultra-wideband ranging: A particle filter approach. *Elsevier Robotics and Autonomous Systems* 57(5):496-507

Habash, M.F., Tantawy, A.S., Atallah, H.A. & Rahman, A.B.A. 2018. Compact size triple notched-bands uwb antenna with sharp band-rejection characteristics at wimax and wlan bands. *Advanced Electromagnetic* 7(3):99-103.

Jiang, S., Miraslow, J.S., Yuan, Y., Sun, C. & Lu, Y. 2011. Ultra-wideband applications in industry:a critical review. *Taylor & Francis Journal of Civil Engineering and Management* 17(3): 437-444.

Jainal, S.F., Mohamed, N., & Hamzah, A. 2019 Design of ultra-wideband planar antenna characterized of a notched band for wireless local area network. *Symposium SOFTT (Symposium of Future Telecommunication Technologies) 2019,* 1-4.

Jainal, S.F., Mohamed, N., & Hamzah, A. 2019. Band rejection for wlan utilizing ultra-wideband planar antenna. *Conference MJWRT (Malaysia-Japan Workshop on Radio Technology) 2019,* 1-4.

Jainal, S.F., Mohamed, N. & Hamzah, A. 2018. A configuration of ultra-wideband planar antenna comprises band suppression

at 5~6 and 3.3~3.7GHz. *International Journal of Integrated Engineering (IJIE)* 10(7):233-243.

Kadri, A., Jiang, J. & Rao, R.K. 2011. Experimental evaluation of wideband signals-based wireless sensor networks for industrial environments. *Proceedings IWCMC (7th International Wireless Communications and Mobile Computing 2011,* 1341-1346.

Khan, M.I., Khattak, M.I., Witjaksono, G., Barki, Z.U., Ullah, S., Khan, I. & Lee, B.M. 2019. Experimental investigation of a planar antenna with band rejection features for ultra-wide band (uwb) wireless networks. *International Journal of Antennas and Propagation 2019:1-11.*

Khattak, M.I., Khan, M.I., Ullah, Z., Ahmad, G. & Khan, A. 2019. Hexagonal printed monopole antenna with triple stop bands for uwb applications. *Mehran University Research Journal of Engineering & Technology* 38(2):335-340.

Kheiri, F., Dewberry, B., Jackson, A. & Joiner, L.L. 2008. Impulse ultra-wideband ad-hoc tracking and communication network. *Conference MILCOM (IEEE Military Communication) 2008,* 1-7.

Kumar, S. & Khan, T. 2019. Ebg-loaded dielectric resonator antenna for triple characteristics. *Conference AP-RASC (URSI Asia-Pacific Radio Science 2019*,1-5.

Kumar, O.P., Singh, A., Sinha, R. & Ali, T. 2019. Acs fed triple band notched uwb antenna for diverse wireless applications. *International Journal of Innovative Technology and Exploring Engineering (IJITEE)* 8(7):1471-1476.

Maalek, R. & Sadeghpour, F. 2013. Accuracy assessment of ultra-wideband technology in tracking static resources in indoor construction scenarios. *Elsevier Automation in Construction* 30:170-183.

Mohamed, S.S., Majed, O.A.D., Amjad, Y.H., Ziad, A. 2019. A compact ultra-wideband patch antenna with dual band-notch performance for wimax/wlan services. *IEEE Jordan International Joint Conference on Electrical Engineering and Information Technology (JEEIT),* 831-834.

Phunchongharn, P., Niyato, D., Hossain, E. & Camorlinga, S. 2010. An emi-aware prioritized wireless access scheme for e-health applications in hospital environments. *IEEE Transactions on Information Technology in Biomedicine* 14(5):1247-1258.

Siddiqui, H., Vahdatikhaki, F. & Hammad, A. 2019. Case study on application of wireless ultra-wideband technology for tracking equipment on a congested site. *Journal of Information Technology in Construction* 24(2019):167-187.

Wang, S., Dong, J. & Wang, M. 2019. A frequency-reconfigurable uwb antenna with switchable single/dual/triple band notch functions. *Cross Strait Quad-Regional Radio Science and Wireless Technology Conference (CSQRWC)* 1-3.

Xu, L., Xiao, X. & Kikkawa, T. 2013. Ultra-wide band microwave image reconstruction image reconstruction for early breast cancer detection by norm constrained capon beamforming. *Elsevier Journal of Mathematical and Computer Modeling* 58(1-2):403-408.